

RESEARCH

Open Access



Shape recovery properties of 3D printed re-entrant strip using shape memory thermoplastic polyurethane filaments with various temperature conditions

Imjoo Jung¹ and Sunhee Lee^{2*}

*Correspondence:
shlee014@dau.ac.kr

¹ Department of Fashion and Textiles, Dong-A University, Busan 49315, Republic of Korea

² Department of Fashion Design, Dong-A University, 37 Nakdong-Daero, Saha-Gu, Busan 49315, Republic of Korea

Abstract

In this research, to confirm the applicability as the actuator of the re-entrant (RE) structure strip using 3D printing with shape memory thermoplastic polyurethane material, two types of 3D printing infill conditions and five extension temperature conditions were applied. REstrip was analyzed through differential scanning calorimetry (DSC), tensile properties, Poisson's ratio properties, and shape recovery properties according to temperature conditions. The DSC results showed that the glass transition temperature peaks of the SMTPU filament and the 3D printed REstrip were in the range of about 30–60 °C. In terms of tensile properties, the initial modulus, maximum stress, and yield stress of REstrip all decreased, while the elongation at break increased with increasing extension temperature. In terms of Poisson's ratio, it was confirmed that as the extension temperature rises, Poisson's ratio shows a positive value at a lower elongation, and the deformation is best at 50 °C. As a result of the shape memory property, the shape recovery ratio tended to decrease as the tensile deformation temperature increased.

Keywords: Shape memory thermoplastic polyurethane, 3D printing, Re-entrant, Extension temperature, Shape recovery property

Introduction

Shape memory polymers (SMP) are materials that can change their shape or physical properties and later restore their original (permanent) state in response to external stimulation such as electricity, magnetic stimulation, moisture, temperature, light, etc. In recent years, such materials have also come to be called smart materials or programmable materials, and they have been applied in fields such as biomedicine, aerospace, intelligent textiles, actuators, and sensors. Thermo-responsive SMP exhibits shape change and recovery phenomena in a specific temperature range between the glass transition temperature (T_g) and the melting temperature (T_m), mainly by applying the T_g temperature (Momeni et al., 2017; Sun et al., 2013). In particular, thermoplastic polyurethane (TPU) is widely used among SMPs due to their soft, elastic, and wide

T_g range. TPU is a multi-block copolymer that is glassy at temperatures below the T_g and rubbery at temperatures above the T_g . TPU can exhibit this behavior because it consists of hard and soft segments. The hard segments fix the phase through physical crosslinking and provide strength, while the soft segments can restore the phase and offer flexibility (Drobny, 2014). Through these properties, TPU can have shape memory properties. As the SMTPU is a temperature-sensitive type, the setting temperature is a very important parameter. It is possible to set the chemistry and structure in various ways according to the temperature design. Therefore, it is very important to find suitable temperature conditions according to the purpose (Lendlein & Kelch, 2002; Xie, 2011). In the bio-medical field, research is being conducted to confirm manufacturing conditions suitable for body temperature or to confirm suitable temperature conditions when manufacturing actuators that can be applied to various fields (Ramezani & Monroe, 2022; Song et al., 2015a, 2015b; Zeng et al., 2020). Accordingly, the SMTPU is manufactured by synthesizing various materials to improve performance (Park et al., 2014; Patel & Purohit, 2019).

The temperature-sensitive SMTPU is manufactured as a filament, applied the FFF (Fused Filament Fabrication) 3D printing, and printed in various forms. The FFF 3D printing process is a printing method by melting a filament. Recently, they are moving further to 4D printing method by utilizing SMTPU performance (Garces & Ayranci, 2021; Salimon et al., 2020). 4D printing is a technology that allows 3D printed objects to change their physical properties and shape over time (Momeni et al., 2017). These SMTPUs are being developed into filaments by synthesizing various materials such as PLA (polylactic acid), PANI (polyaniline), PPC (polypropylene carbonate), PCL (polycaprolactone), and CIP (carbonyl iron particles) based on TPU. The manufactured filaments are printed in various shapes and then subjected to shape recovery experiments (Carlson and Li, 2020; Monzon et al., 2017; Qi et al., 2019; Wang et al., 2022). In addition, various studies have diversified materials and modeled structures for 4D printing, and thus developed materials with excellent shape recovery performance.

In particular, the re-entrant (below RE) pattern of the auxetic structures is a structure formed by two sides with an inward negative angle in the form of a 'bowtie'. Due to the inward sides, the RE pattern exhibits auxetic behavior when stretched or compressed. RE structures exhibit superior physical properties such as pressure resistance, energy absorption, and toughness compared to other auxetic structures (Lakes, 2017; Li et al., 2020). In recent years, smart sensors, actuators, and metamaterials have been developed by applying the characteristics of such auxetic structures. There have also been attempts to design structures for 4D printing implementation. Among research applying auxetic structures for 4D printing to develop shape memory materials, there are several studies in which chiral structures were printed by the FDM process using PLA/TPU/CNT (carbon nanotube) filaments (Dong et al., 2021), wherein RE structures were fabricated with photocurable resins and SLA (stereolithography) processes (Pandini et al., 2019; Pasini et al., 2022). Kabir et al. (2020) and Kabir and Lee (2020) reported samples that applied a sinusoidal structure and were printed using TPU and SMTPU filaments. Further, its physical properties were confirmed by shape memory cycle and applied to shoe uppers. Jung et al. (2022a) studied the most suitable modeling for the hand movements of a robot hand. A finger was modeled with two modelings of a cap type and

a strip type to which the RE structure was applied, a programming of a four-type finger movement control system was created, and the movement functionality was evaluated. It was confirmed that the strip type-applied RE structure was suitable for grasping hand manipulation.

Our research team is conducting research to develop 4D printing metastructure soft actuator for healthcare applications. In particular, materials and modeling are very important factors in manufacturing soft actuators that are soft, flexible, and have no sense of heterogeneity in the movement of the human body. Therefore, our research is underway materials based on soft and elastic TPU and auxetic structures among metastructures. To this end, we are proceeding with preliminary studies related to TPU (Kim & Lee, 2020; Jung et al., 2022b; Shin et al., 2022a, 2022b) and SMTPU (Jung et al., 2023). Further, there is previous research into the development and performance evaluation of TPU/textile composite fabrics (Jung et al., 2021; Kim et al., 2021) applied TPU and RE structures. In terms of studies applying SMTPU and RE structures, the previously referenced studies by Kabir et al. (2020) and Kabir and Lee (2020) confirmed the shape memory properties of a sinusoidal structure using SMTPU. As a previous study for sensor and actuator fabrication, Choi et al. (2022) and Choi et al. (2023) manufactured a TPU strain sensor and piezo-resistive sensor coated CWPU (caster-oil-based waterborne polyurethane)/graphene. And Jung et al. (2022a) studied finger modeling suitable for hand movements and confirmed that the REstrip is suitable. Through previous studies, it was confirmed that the TPU material and the RE structure had excellent performance in manufacturing 3D printed soft actuators.

Therefore, in this study, the most suitable 3D printing infill patterns and temperature conditions were confirmed when the REstrip is used for an temperature-responsive actuator acting as a muscle applied on wearable smart gloves. According to the results of previous study (Jung et al., 2022a, 2022b), the 3D printed actuator used a REstrip shape suitable for the grasping motion of the hand. REstrip was manufactured using a temperature-responsive SMTPU applied two types of infill patterns that divided layer into lines and shapes. First, the SMTPU and 3D printed REstrip were identified in thermal property evaluation to set the temperature conditions. Based on the results of the thermal property analysis, five temperature conditions were set. In addition, the tensile properties and Poisson's ratio during constant extension were confirmed. Further, the constant extended REstrip was performed to shape recovery experiment for 5 min while applying an initial load of 1 g at a temperature of 70 °C. Lastly, the shape recovery properties were analyzed.

Experimental

Materials

In this study, shape memory thermoplastic polyurethane (SMTPU) was used to fabricate REstrips. SMTPU (SMP Technologies Inc., Japan) filament was manufactured with a diameter of 1.75 mm for the 3D printing process, and a transparent color was used.

Preparation of 3D printed REstrip

To begin, a conceptual 2D RE pattern was developed with a repeating unit of 12×12 mm². This repeating unit was combined and transformed to a strip. 2D modeling was



Fig. 1 Image of 3D printed REstrip

Table 1 Sample code of 3D printed REstrip

| Sample code | Infill pattern | Infill density (%) | Extension temp. (°C) | Sample code | Infill pattern | Infill density (%) | Extension temp. (°C) |
|-------------|----------------|--------------------|----------------------|-------------|----------------|--------------------|----------------------|
| ZG-100-30 | Zigzag | 100 | 30 | TR-100-30 | Triangle | 100 | 30 |
| ZG-100-50 | | | 50 | TR-100-50 | | | 50 |
| ZG-100-60 | | | 60 | TR-100-60 | | | 60 |
| ZG-100-70 | | | 70 | TR-100-70 | | | 70 |
| ZG-100-90 | | | 90 | TR-100-90 | | | 90 |

performed with the Illustrator CC (Adobe, USA) program. Then, 3D modeling with the dimensions of $12.0 \times 178.4 \times 2.0 \text{ mm}^3$ was conducted in Fusion 360 (Autodesk Co. Ltd., USA) program to create a.stl file. The.stl file was converted to 3D printable g-code file by Cubicreator 4.4 (Cubicon Co. Ltd., Korea) program. Next, REstrip was printed using an FDM 3D printer (Cubicon single plus, Cubicon Co. Ltd., Korea) with a nozzle with a diameter of 0.4 mm. The conditions for 3D printing were set to a nozzle temperature of 235 °C, a bed temperature of room temperature, a printing speed of 50 mm/s, an infill pattern of Zigzag (below ZG) and Triangle (below TR), and an infill density of 100%. In addition, the 3D printing environment maintained room temperature and humidity below 50%. The 3D printed samples were stored in a desiccator (Desiccator Auto C-3B, Sanplatec corp., Japan) for humidity control. In case of infill pattern, the ZG and TR are 2D and 3D infill types that divide layers into lines and figures. Among the 2D infill types, ZG consists of one line in which all lines are connected in one layer, forming an outline. The 3D infill type TR is a pattern in which lines in three directions form a 60° angle and move while drawing a triangle. ZG and TR patterns show soft-toughness as the infill density increases. And in particular, the process time is the shortest in the case of ZG (Jung & Lee, 2022). Figure 1 shows an image of a 3D printed REstrip and Table 1 presents the REstrip’s sample code.

Shape recovery test conditions

Figure 2 shows the shape recovery test conditions for REstrip. The shape recovery test was conducted in three steps. Step 1 was the stage of preparing REstrip by 3D printing. The sample was prepared with the dimensions of $12 \times 130 \times 2 \text{ mm}^3$. Step 2 conducted a constant extension using a universal testing machine (AGS-500D, Shimadzu, Japan) and a hot chamber (TemcoLine, Korea). After 100% stretching under the temperature conditions of 30 °C, 50 °C, 60 °C, 70 °C, and 90 °C, the length was fixed and stored at room temperature. The tensile speed was 50 mm/min and the gauge length was set to 50 mm.

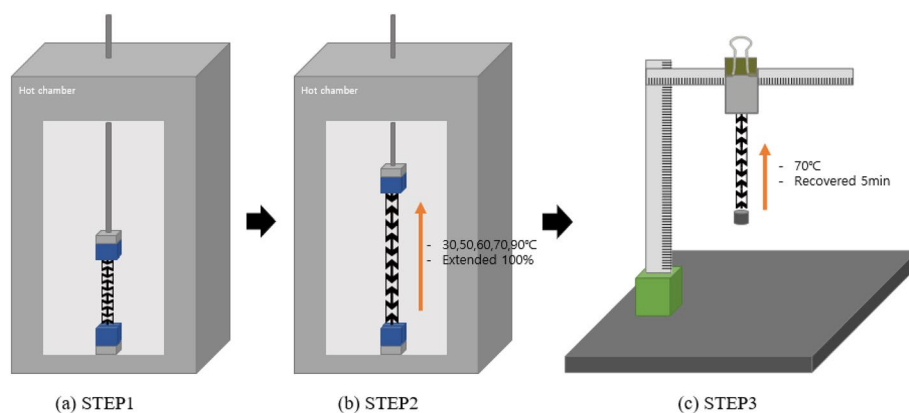


Fig. 2 Shape recovery test of REstrip

Step 3 was the state of recovering the shape of the sample that was extended in step 2. A shape recovery test was performed in a temperature of 70 °C for 5 min. At this time, an initial load of 1 g was applied, and the recovered sample was stored at room temperature for 24 h.

Characterizations

Differential scanning calorimetry

For thermal analysis of SMTPU filaments and 3D printed REstrip, a DSC analyzer (DSC25, TA instruments, USA) was used with a heating rate of 10 °C/min and a measurement range of 20–300 °C. DSC curves were also obtained. Moreover, the glass transition temperature and melting temperature were confirmed. The sample amount was 2.5 mg.

Tensile property

To confirm the tensile properties of REstrip under various temperature conditions, a universal testing machine (AGS-500D, Shimadzu, Japan) and a hot chamber (TemcoLine, Korea) were used. Each sample was prepared in dimensions of $12.0 \times 100.5 \times 2.0 \text{ mm}^3$ under the five temperature conditions of 30 °C, 50 °C, 60 °C, 70 °C, and 90 °C. The gauge length and the tensile speed progressed at 25 mm and 25 mm/min, respectively. Through a tensile test, stress–strain (S–S) curves were obtained to measure initial elastic modulus, maximum stress, elongation at break, and yield stress. The measured data were analyzed to determine the tensile properties under various temperature conditions. To investigate this difference, the SPSS 27.0 statistical program was used to perform one-way ANOVA. For all analyses, the significance level was set at $p < 0.05$.

Poisson's ratio

Poisson's ratio was measured using a universal material testing machine (AGS-500D, Shimadzu, Japan) and a hot chamber (TemcoLine, Korea) to confirm the auxetic properties of REstrip under constant extension deformation with various temperature conditions. The measurement positions are shown in Fig. 3. The sample was prepared with dimensions of $12 \times 130 \times 2 \text{ mm}^3$. The temperature conditions were set at 30 °C,

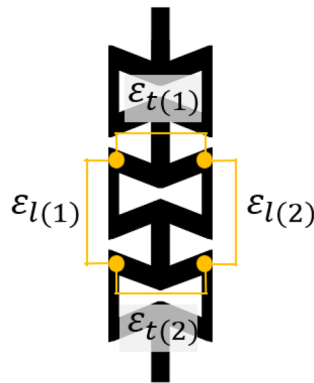


Fig. 3 Measurement position of Poisson's ratio

50 °C, 60 °C, 70 °C, and 90 °C. The gauge length and tensile speed were 50 mm and 50 mm/min, respectively. During the tensile experiments, experimental video was taken using a digital camera (VCXU-123 M.K06, GOM, Germany) using the Gom snap 2D 2020 (GOM, Germany) program. Further, the strain of the sample was calculated using the Gom Correlate 2020 (GOM, Germany) program. Lastly, Poisson's ratio was obtained through Eq. (1).

$$\nu = -\varepsilon_t / \varepsilon_l \tag{1}$$

where ν indicates Poisson's ratio, ε_t is the average transverse strain, and ε_l is the average axial strain.

Shape recovery properties

For the shape recovery properties of the REstrip, the sample length and the shape recovery ratio for each stage were confirmed after the recovery experiment. The shape recovery ratio of the REstrip sample is calculated using Eq. (2) compared to the sample length obtained in step 1 and the sample length recovered in step 3.

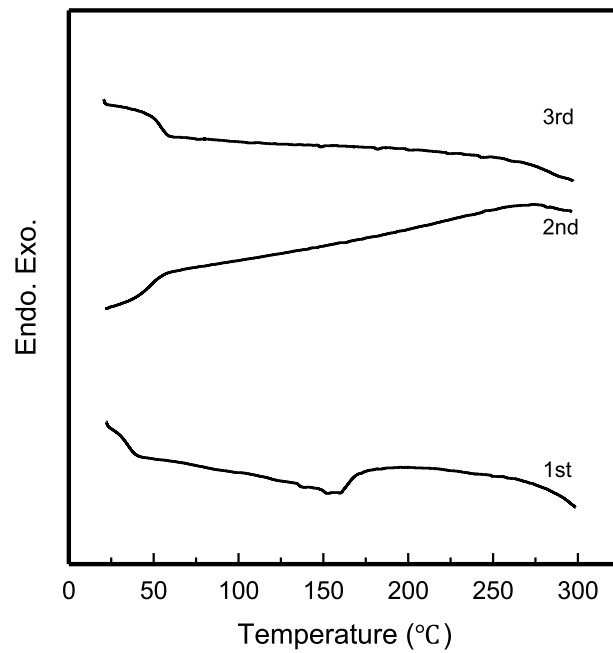
$$R(\%) = \left(\varepsilon - \frac{\varepsilon_{rec}}{\varepsilon} \right) \times 100 \tag{2}$$

here, R is the shape recovery ratio, ε is the sample length of step 1, and ε_{rec} is the length of the sample after step 3.

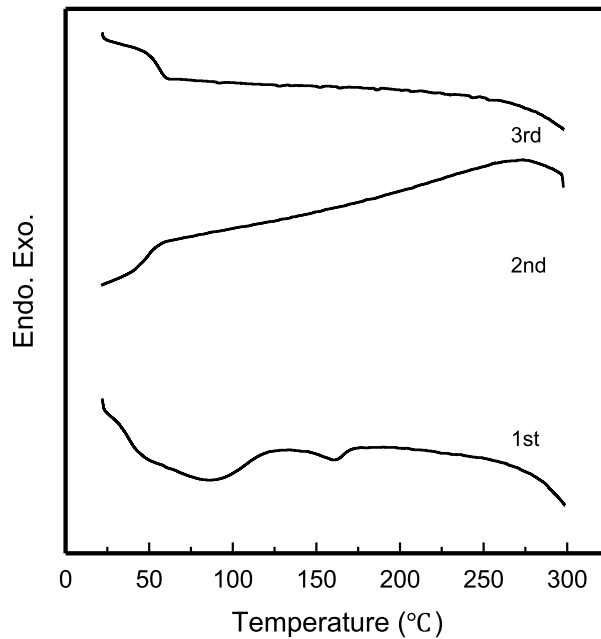
Results and Discussion

Thermal properties of SMTPU filament and 3D printed REstrip

Figure 4 shows the DSC curves of the SMTPU filament and the 3D-printed REstrip, while Table 2 lists the glass transition temperature (T_g), the melting temperature (T_m), the crystallization temperature (T_{cc}), and the enthalpy (ΔH) value characteristic temperature. Samples were measured to a 1st–3rd curve to compare the temperatures of the SMTPU filament and post 3D printed REstrip. In general, the 1st curve shows the thermal properties of the sample as it is, the 2nd curve shows the crystallization peak when the melted sample is cooled, and the 3rd curve shows the thermal properties without processing or finishing.



(a)



(b)

Fig. 4 DSC curve; (a) SMTPU filament and (b) 3D printed REstrip

In the case of the SMTPU filament, the 1st curve showed that the T_g appeared in the range from 30.0 to 60.0 °C with a peak at 40.0 °C. The T_m appeared from 140.0 °C, peaked at 160.0 °C, and ΔH was confirmed to be 7.3 J/g. In the 2nd curve, as the T_{cc} was in the range from 50.0 to 70.0 °C and the peak appeared at 56.4 °C, it is confirmed

Table 2 Thermal properties of SMTPU filament and 3D printed REstrip

| Sample | | Tg* (°C) | Tm** (°C) | Tcc*** (°C) | ΔH (J/g) |
|----------------|-----|----------|-----------|-------------|----------|
| SMTPU filament | 1st | 40.1 | 160.0 | – | 7.3 |
| | 2nd | – | – | 56.4 | 2.7 |
| | 3rd | 59.7 | – | – | – |
| REstrip | 1st | 80.0 | 161.4 | – | 1.6 |
| | 2nd | – | – | 54.9 | 2.1 |
| | 3rd | 60.5 | – | – | – |

*Tg: Glass transition temperature

**Tm: Melting temperature

***Tcc: Cold crystallization temperature

that the internal structure was uniform. In the 3rd curve, the T_g appeared at about 60 °C, similar to the 1st curve, and the T_m did not appear. In the case of REstrip, it was represented by one data as ZG-100, and TR-100 showed the same tendency. The 1st curve showed a T_g in the range from 30.0 to 120.0 °C with a peak at 80.0 °C. It was confirmed that, as moisture was included during 3D printing, the range of the peak was represented widely. The T_m appeared at 140.0 °C with a peak at 161.0 °C, and ΔH was confirmed to be 1.6 J/g. The 2nd curve showed a T_{cc} range from 40.0 to 70.0 °C with a peak at 54.9 °C. In the 3rd curve, the T_g was 60 °C and the T_m peak did not appear.

Therefore, SMTPU filaments and REstrips were identified as showing similar results and as having uniform thermal properties in the 1st–3rd curves. Moreover, since REstrip shows a moisture peak in the 1st curve, it was confirmed that it is necessary to perform pretreatments such as drying and crystallization before the preparation of the sample to use it. Based on the DSC results, the extension temperature was then set from 30 to 90 °C according to the glass transition temperature.

Tensile properties of ZG-100 and TR-100 of 3D printed REstrip with various extension temperatures

Figure 5 shows S–S curves with various extension temperatures of ZG-100 and TR-100, while Table 3 lists tensile properties such as initial modulus, elongation at break, maximum stress, and yield stress.

As shown in Fig. 5, the initial modulus showed a tendency to decrease sharply as the extension temperature increased from room temperature (R.T.) to 90 °C. The breaking elongation increased from 103.3% to 934.0% for ZG-100 and from 120.1% to 997.5% for TR-100. The maximum stress decreased from 0.38 MPa to 0.00 MPa for ZG-100 and from 0.43 MPa to 0.00 MPa for TR-100. It was therefore found that the higher the extension temperature, the greater the elongation and the lower the stress when the sample was extended.

As can be seen in Table 3, for the initial modulus, when the extension temperature increased from R.T. to 90 °C, ZG-100 was 2.70 MPa, 1.84 MPa, 0.29 MPa, 0.03 MPa, 0.01 MPa, and 0.00 MPa, and TR-100 was 3.57 MPa, 2.22 MPa, 0.21 MPa, 0.03 MPa, 0.01 MPa, and 0.01 MPa. It was confirmed that the initial modulus had a tendency to be higher for TR-100, and the difference was particularly large between R.T. and

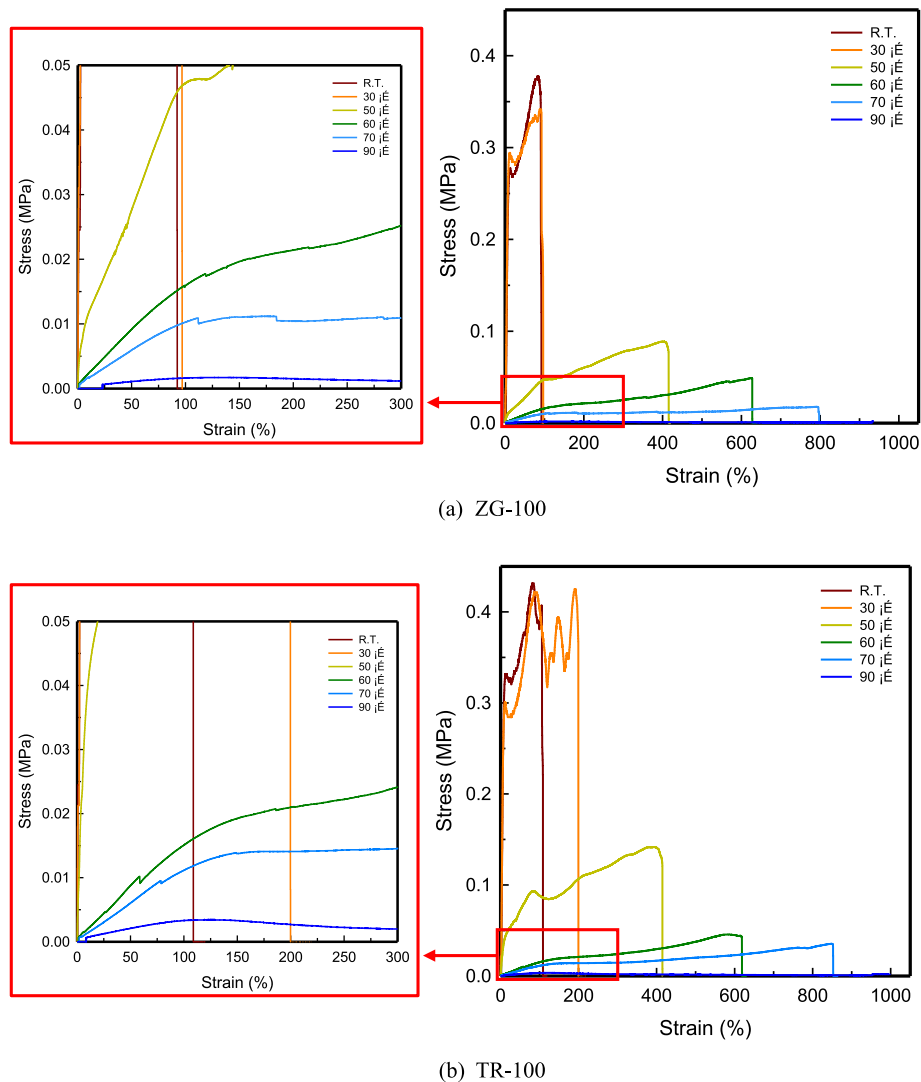


Fig. 5 Stress-strain curves of ZG-100 and TR-100 of REstrip with various extension temperatures

30 °C. For breaking elongation, with increasing extension temperature, ZG-100 showed values of 111.96%, 184.87%, 330.08%, 598.56%, 776.64%, and 938.10%, and TR-100 showed values of 101.63%, 176.55%, 408.04%, 648.50%, 831.46%, and 987.26%. It showed a similar tendency between ZG-100 and TR-100, but it was confirmed that TR-100 has a greater elongation at break at more than 50 °C. The maximum stress was found to be 0.39 MPa, 0.35 MPa, 0.09 MPa, 0.07 MPa, 0.02 MPa, and 0.00 MPa for ZG-100, and 0.42 MPa, 0.40 MPa, 0.16 MPa, 0.03 MPa, 0.03 MPa, and 0.03 MPa for TR-100. The yield strength of ZG-100 was 0.28 MPa, 0.28 MPa, 0.05 MPa, 0.03 MPa, 0.01 MPa, and 0.00 MPa, and that of TR-100 was 0.37 MPa, 0.31 MPa, 0.10 MPa, 0.03 MPa, 0.03 MPa, 0.00 MPa, and 0.00 MPa. Therefore, similar to the initial modulus, the maximum stress and yield stress decreased with increasing extension temperature. Further, TR-100 tended to be greater than ZG-100. Moreover, it was confirmed

Table 3 Tensile properties of ZG-100 and TR-100 of 3D printed REstrip with various extension temperatures

| Sample | Extension temp. (°C) | R.T | 30 | 50 | 60 | 70 | 90 | F |
|--------|-----------------------------|----------------|----------------|----------------|----------------|----------------|----------------|------------|
| ZG-100 | Initial modulus (MPa) | 002.70 ± 00.02 | 001.84 ± 01.24 | 000.29 ± 00.32 | 000.03 ± 00.01 | 000.01 ± 00.00 | 000.00 ± 0.00 | 9.969** |
| | Breaking elongation (%) | 111.96 ± 12.22 | 184.87 ± 92.02 | 385.50 ± 50.21 | 598.56 ± 60.19 | 776.64 ± 55.72 | 938.10 ± 5.80 | 41.841*** |
| | Stress _{max} (MPa) | 000.39 ± 00.01 | 000.35 ± 00.01 | 000.09 ± 00.00 | 000.07 ± 00.03 | 000.02 ± 00.00 | 000.00 ± 0.00 | 27.397*** |
| | Yield stress (MPa) | 000.28 ± 00.00 | 000.28 ± 00.01 | 000.05 ± 00.00 | 000.03 ± 00.01 | 000.01 ± 00.00 | 000.00 ± 0.00 | 23.926*** |
| TR-100 | Initial modulus (MPa) | 003.57 ± 00.52 | 2.22 ± 1.06 | 000.21 ± 00.06 | 000.03 ± 00.01 | 0.01 ± 0.00 | 000.01 ± 00.01 | 19.903** |
| | Breaking elongation (%) | 101.63 ± 26.06 | 176.55 ± 60.51 | 408.04 ± 37.96 | 648.50 ± 24.75 | 831.46 ± 48.23 | 987.26 ± 14.45 | 171.267*** |
| | Stress _{max} (MPa) | 000.42 ± 00.01 | 0.40 ± 0.04 | 000.16 ± 00.02 | 000.06 ± 00.01 | 0.03 ± 0.01 | 000.00 ± 00.00 | 181.235*** |
| | Yield stress (MPa) | 000.37 ± 00.06 | 0.31 ± 0.01 | 000.10 ± 00.01 | 000.03 ± 00.01 | 0.01 ± 0.00 | 000.00 ± 00.00 | 90.034*** |

p < 0.05, *p < 0.005

that the tensile properties statistically differed depending on the temperature conditions and exhibited significant differences ($p < 0.01$, $p < 0.001$).

As the extension temperature rises, the initial modulus, maximum stress, and yield stress all tend to increase, and the breaking elongation tends to decrease, implying that temperature-responsive shape memory polymers deform more easily at higher temperatures and require less load to deform. Therefore, there will be little stress at 90 °C, which is above the glass transition temperature range (Fritzsche & Pretsch, 2014; Pasini et al., 2022). Further, the tendency of TR-100 to be superior to ZG-100 in terms of tensile properties can be inferred from the shape of the infilled pattern. In the case of the Triangle pattern, the layers are deposited in three directions forming a 60° angle. The zigzag pattern stacked the layers in two directions intersecting at right angles, as it consisted of one layer of lines in one direction (Jung & Lee, 2021). During 3D printing, this was printed in the z-axis direction. However, in this study, the sample was extended while being applied in the direction perpendicular to the printing direction. Thus, the strength of TR-100, which was deposited in three directions, appeared better.

Poisson’s ratio of ZG-100 and TR-100 of 3D printed REstrip with various extension temperatures

Figure 6 shows the Poisson’s ratio for ZG-100 and TR-100 at 100% elongation with various extension temperatures.

Poisson’s ratio describes the ratio of horizontal strain and vertical strain that deforms when a material is loaded in one direction, such as tension or compression. For both ZG-100 and TR-100, the largest range of Poisson’s ratio appeared at the extension temperature of 30 °C. The positive Poisson’s ratio exhibited elongation of 78%, 40%, 53%, 48%, and 38% for ZG-100 and 48%, 40%, 50%, 50%, and 40% for TR-100 with increasing

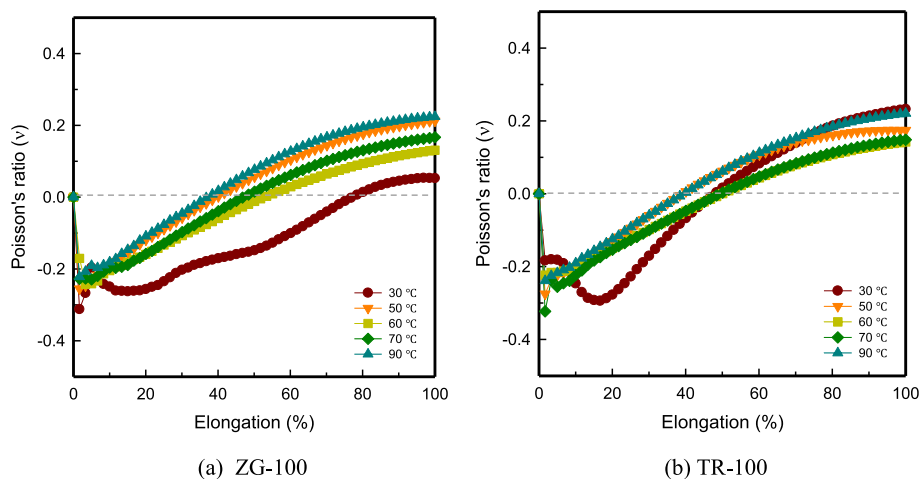


Fig. 6 Poisson's ratio of samples under 100% extension with various extension temperatures

extension temperature. As the extension temperature increased, the elongation appeared to have a positive Poisson's ratio that tended to decrease. However, when the extension temperature was 50 °C, the positive value was shown at a lower elongation than 60 °C and 70 °C. Therefore, it was confirmed that the morphology changed well at an extension temperature of 50 °C. Moreover, as the Poisson's ratio values exhibited a range from − 1 to 1 for both ZG-100 and TR-100, they exhibited auxetic properties over the entire extension temperature range.

Shape recovery properties of ZG-100 and TR-100 of 3D printed REstrip with various extension temperatures

Table 4 presents sample images taken after the shape recovery test with various extension temperatures, Fig. 7 is a graph showing the shape recovery ratio, and Table 5 shows RE structures images after shape recovery testing.

The length of the specimen recovered at 70 °C for 5 min after extension was 37.5 mm, 37.0 mm, 39.0 mm, 45.0 mm, and 68.5 mm for ZG-100 and 37.0 mm, 37.3 mm, 39.5 mm, 44.3 mm, and 61.7 mm for TR-100 as the extension temperature increased from 30 °C to 90 °C. As a result of calculating the shape recovery ratio by comparing the recovered sample length with the initial length of the sample of 36.0 mm, the results were identified to be 95.8%, 97.2%, 91.7%, 75.0%, and 9.7% for ZG-100 and 97.2%, 97.2%, 90.3%, 76.9%, and 28.7% for TR-100. Therefore, it was confirmed that, as the extension temperature increases, the shape recovery ratio decreases. The infill pattern did not show a large difference, but the shape recovery ratio of TR-100 showed a tendency to be slightly better. In addition, as the shape recovery ratio appeared to be 90% or more at an extension temperature of 30–60 °C, the REstrip could recover a similar initial state. When the temperature is above the T_g , physical cross-links of the soft part and the hard part can partly deform or disappear (Drobny, 2014). Thus, at the extension temperature of 90 °C, it seems that the shape recovery ratio was 9.7% for ZG-100 and 28.7% for TR-100.

The shape recovery property of the RE structure was confirmed by the change in the length of the repeating unit after recovery for 5 min. Step 1 was the same for one repeat unit of the RE structure of 12.0 mm. As the extension temperature increased from 30 °C

Table 4 Sample recovery images of 3D printed REstrip under constant extension with various extension temperatures

| Sample code | ZG-100-30 | | | ZG-100-50 | | | ZG-100-60 | | | ZG-100-70 | | | ZG-100-90 | | |
|-------------|-----------|----------|----------|-----------|----------|----------|-----------|----------|----------|-----------|----------|----|-----------|----|--|
| | Step | 2 | 3 | 2 | 3 | 70 | 2 | 3 | 70 | 2 | 3 | 70 | 2 | 3 | |
| Temp. (°C) | R.T | 30 | 70 | 50 | 70 | 70 | 60 | 70 | 70 | 70 | 70 | 70 | 90 | 70 | |
| Images | | | | | | | | | | | | | | | |
| Length (mm) | 36.0±0.0 | 64.0±0.0 | 37.0±0.0 | 70.5±0.7 | 37.3±0.6 | 71.0±1.4 | 39.5±0.5 | 75.0±0.0 | 40.1±0.8 | 78.5±0.7 | 61.7±3.8 | | | | |
| Sample | TR-100-30 | | | TR-100-50 | | | TR-100-60 | | | TR-100-70 | | | TR-100-90 | | |
| Step | 1 | 2 | 3 | 2 | 3 | 70 | 2 | 3 | 70 | 2 | 3 | 70 | 2 | 3 | |
| Temp. (°C) | R.T | 30 | 70 | 50 | 70 | 70 | 60 | 70 | 70 | 70 | 70 | 70 | 90 | 70 | |
| Images | | | | | | | | | | | | | | | |
| Length (mm) | 36.0±0.0 | 65.0±0.0 | 37.5±0.7 | 71.7±0.6 | 37.0±0.0 | 73.3±0.6 | 39.0±0.0 | 74.0±0.0 | 45.0±1.4 | 75.0±0.0 | 68.5±2.1 | | | | |

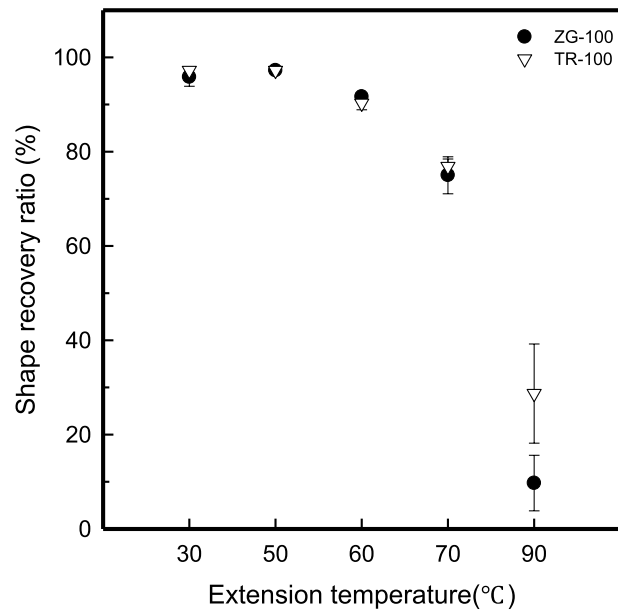











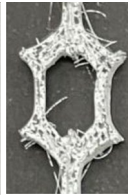


Fig. 7 Shape recovery ratio of 3D printed REstrip under extension with various extension temperatures

Table 5 Sample recovery images of RE structure under constant extension with various extension temperatures

| Sample code | ZG-100 | ZG-100-30 | ZG-100-50 | ZG-100-60 | ZG-100-70 | ZG-100-90 |
|-------------|---|---|---|--|---|---|
| Step | 1 | 3 | | | | |
| Temp. (°C) | R.T | 70 | | | | |
| Images |  |  |  |  |  |  |
| Length (mm) | 12.0±0.0 | 12.5±0.7 | 13.0±0.0 | 13.8±0.4 | 16.5±0.7 | 25.0±0.0 |
| Sample code | TR-100 | TR-100-30 | TR-100-50 | TR-100-60 | TR-100-70 | TR-100-90 |
| Step | 1 | 3 | | | | |
| Temp. (°C) | R.T | 70 | | | | |
| Images |  |  |  |  |  |  |
| Length (mm) | 12.0±0.0 | 12.8±0.4 | 13.0±0.0 | 13.3±0.4 | 15.5±0.7 | 22.0±1.4 |

to 90 °C, the recovered length of the RE structure was 12.5 mm, 13.0 mm, 13.8 mm, 16.5 mm, and 25.0 mm for ZG-100 and 12.8 mm, 13.0 mm, 13.3 mm, 15.5 mm, and

22.0 mm for TR-100. It was shown that, the higher the extension temperature, the lower the shape recovery ratio. It was also confirmed that the RE structure recovered similarly to the range at 30–60 °C and had auxetic properties similar to REstrip.

Conclusions

In this study, to confirm the applicability of 3D printed REstrip as an actuator, its thermal properties, tensile properties, Poisson's ratio, and shape recovery properties were confirmed. The DSC results showed that the T_g peaks of the SMTPU filament and the 3D printed REstrip appeared in the range from about 30–60 °C. Therefore, the extension temperature was set at 30–90 °C. Moreover, the shape recovery temperature was set at 70 °C, which is higher than T_g . In terms of tensile strength, the initial modulus, maximum stress, and yield stress of the REstrip decreased, and the breaking elongation increased with increasing extension temperature. At R.T. – 30 °C, TR-100 was superior to ZG-100 in terms of tensile properties. Although no significant difference was observed at 50–90 °C, there was generally a tendency that TR-100 had a higher strength than ZG-100. In the case of Poisson's ratio, it showed the largest range at 30 °C. Further, at 90 °C, the Poisson's ratio showed a positive value at the lowest elongation. Moreover, it was confirmed that the deformation is best at 50 °C. As a result of the shape recovery properties, the shape recovery ratio decreased as the extension temperature increased, and the infill pattern showed a similar tendency. Therefore, the infill pattern of TR and temperature condition of 50 °C—which is easy to deform and has a high shape recovery ratio—were confirmed as an appropriate manufacturing conditions for actuator. Therefore, based on the results, temperature-responsive REstrip is intended to be developed as a strain actuator applied to wearable smart gloves that can be assist stroke, spinal cord injury, and cerebral palsy patient's rehabilitation as acting a muscle. In future research, we plan to use SMTPU which is being developed by our research team and develop an actuator that can be directly applied in a temperature range suitable for the human body. In addition, we will proceed with quantitative measurement of the shape recovery force.

Acknowledgements

Not applicable.

Authors' information

Imjoo Jung, Graduate Student, Department of Fashion and Textiles, Dong-A University, Busan, 49315, Republic of Korea. Sunhee Lee, Professor, Department of Fashion Design, Dong-A University, 37 Nakdong-Daero, Saha-gu, Busan, 49315, Republic of Korea.

Authors' contributions

SL conceived the work and IJ prepared the samples and performed the experiments. IJ and SL are participated in the sequence alignment and drafted the manuscript. Authors read and approved the final manuscript.

Funding

This research was supported by a Grant (No. NFR-2021R1A4A1022059) of the Basic Science Research Program through the National Research (NRF) funded by the Ministry of Science and ICT, Republic of Korea.

Availability of data and materials

The data sets used and analyzed during the current study are available from the corresponding author on reasonable request.

Declarations

Competing interests

The authors declare that they have no competing interests.

Received: 26 December 2022 Accepted: 9 June 2023

Published online: 25 July 2023

References

- Carlson, M., & Li, Y. (2020). Development and kinetic evaluation of a low-cost temperature-sensitive shape memory polymer for 4-dimensional printing. *The International Journal of Advanced Manufacturing Technology*, 106, 4263–4279. <https://doi.org/10.1007/s00170-020-04927-5>
- Choi, H. Y., Shin, E. J., & Lee, S. (2022). Design and evaluation of 3D-printed auxetic structures coated by CWPU/graphene as strain sensor. *Scientific Reports*, 12, 7780. <https://doi.org/10.1038/s41598-022-11540-x>
- Choi, H. Y., Shin, E. J., & Lee, S. (2023). Piezo-resistive Sensor of Auxetic Structures Based on 3D-Printed TPU Coated by Castor-oil Based Waterborne Polyurethane/Graphene. *Fibers and Polymers*, 24, 15–28. <https://doi.org/10.1007/s12221-023-00052-8>
- Dong, K., Panahi-Sarmad, M., Cui, Z., Huang, X., & Xiao, X. (2021). Electro-induced shape memory effect of 4D printed auxetic composite using PLA/TPU/CNT filament embedded synergistically with continuous carbon fiber: A theoretical & experimental analysis. *Composites Part B Engineering*, 220, 108994. <https://doi.org/10.1016/j.compositesb.2021.108994>
- Drobny, J. G. (2014). *Handbook of thermoplastic elastomers* (pp. 233–253). Elsevier.
- Fritzsche, N., & Pretsch, T. (2014). Programming of temperature-memory onsets in a semicrystalline polyurethane elastomer. *Macromolecules*, 47(17), 5952–5959. <https://doi.org/10.1021/ma501171p>
- Garces, I. T., & Ayranci, C. (2021). Advances in additive manufacturing of shape memory polymer composites. *Rapid Prototyping Journal*, 27(2), 379–398. <https://doi.org/10.1108/RPJ-07-2020-0174>
- Jung, I., Kim, H., & Lee, S. (2021). Characterizations of 3D printed re-entrant pattern/aramid knit composite prepared by various tilting angles. *Fashion and Textiles*, 8, 44. <https://doi.org/10.1186/s40691-021-00273-6>
- Jung, I., & Lee, S. (2022). Compressive properties of 3D printed TPU samples. *Journal of the Korean Society of Clothing and Textiles*, 46(3), 481–493. <https://doi.org/10.5850/JKSCT.2022.46.3.481>
- Jung, I., Park, Y., Choi, Y., Kim, J., & Lee, S. (2022a). A study on the motion control of 3D printed fingers. *Textile Science and Engineering*, 24(3), 333–345. <https://doi.org/10.5805/SFTI.2022.24.3.333>
- Jung, I., Shin, E., & Lee, S. (2022b). Morphological characteristics according to the 3D printing extrusion temperature of TPU filaments for different hardnesses. *Textile Science and Engineering*, 59(1), 36–46. <https://doi.org/10.12772/TSE.2022.59.036>
- Jung, Y., Lee, S., Park, J., & Shin, E. (2023). Synthesis of novel shape memory thermoplastic polyurethanes (SMTPUs) from bio-based materials for application in 3D/4D printing filaments. *Materials*, 16, 1072. <https://doi.org/10.3390/ma16031072>
- Kabir, S., Kim, H., & Lee, S. (2020). Physical property of 3D-printed sinusoidal pattern using shape memory TPU filament. *Textile Research Journal*, 90(21–22), 2399–2410. <https://doi.org/10.1177/0040517520919750>
- Kabir, S., & Lee, S. (2020). Study of shape memory and tensile property of 3D printed sinusoidal sample/nylon composite focused on various thicknesses and shape memory cycles. *Polymers*, 12(7), 1600. <https://doi.org/10.3390/polym12071600>
- Kim, H., Kabir, S., & Lee, S. (2021). Mechanical properties of 3D printed re-entrant pattern/neoprene composite textile by pattern tilting angle of pattern. *Journal of the Korean Society of Clothing and Textiles*, 45(1), 106–122. <https://doi.org/10.5850/JKSCT.2021.45.1.106>
- Kim, H., & Lee, S. (2020). Mechanical properties of 3D printed re-entrant pattern with various hardness types of TPU filament manufactured through FDM 3D printing. *Textile Science and Engineering*, 57, 166–176. <https://doi.org/10.12772/TSE.2020.57.166>
- Lakes, R. S. (2017). Negative Poisson's ratio materials: Auxetic solids. *Annual Review of Materials Research*, 47, 63–81. <https://doi.org/10.1146/annurev-matsci-070616-124118>
- Lendlein, A., & Kelch, S. (2002). Shape-memory polymers. *Angewandte Chemistry International*, 41(12), 1973–2208. [https://doi.org/10.1002/1521-3773\(20020617\)41:12%3C2034::AID-ANIE2034%3E3.0.CO;2-M](https://doi.org/10.1002/1521-3773(20020617)41:12%3C2034::AID-ANIE2034%3E3.0.CO;2-M)
- Li, C., Xia, H., Yao, J., & Ni, Q.-Q. (2019). Electrically induced soft actuators based on thermoplastic polyurethane and their actuation performances including tiny force measurement. *Polymer*, 180, 121678. <https://doi.org/10.1016/j.polymer.2019.121678>
- Li, T., Liu, F., & Wang, L. (2020). Enhancing indentation and impact resistance in auxetic composite materials. *Composites Part B Engineering*. <https://doi.org/10.1016/j.compositesb.2020.108229>
- Momeni, F., Liu, X., & Ni, J. (2017). A review of 4d printing. *Materials and Design*, 122, 42–79. <https://doi.org/10.1016/j.matdes.2017.02.068>
- Monzón, M. D., Paz, R., Pei, E., Ortega, F., Suarez, L. A., Ortega, Z., Aleman, M. E., Plucinski, T., & Clow, N. (2017). 4D printing: Processability and measurement of recovery force in shape memory polymers. *The International Journal of Advanced Manufacturing Technology*, 89, 1827–1836. <https://doi.org/10.1007/s00170-016-9233-9>
- Pandini, S., Inverardi, N., Scalet, G., Battini, D., Bignotti, F., Marconi, S., & Auricchio, F. (2019). Shape memory response and hierarchical motion capabilities of 4D printed auxetic structures. *Mechanics Research Communications*. <https://doi.org/10.1016/j.mechrescom.2019.1034>
- Park, J., Dao, T., Lee, H., Jeong, H., & Kim, B. (2014). Properties of graphene/shape memory thermoplastic polyurethane composites actuating by various methods. *Materials*, 7(3), 1520–1538. <https://doi.org/10.3390/ma7031520>
- Pasini, C., Inverardi, N., Battini, D., Scalet, G., Marconi, S., Auricchio, F., & Pandini, S. (2022). Experimental investigation and modeling of the temperature memory effect in a 4D-printed auxetic structure. *Smart Materials and Structures*, 31, 095021. <https://doi.org/10.1088/1361-665X/ac8031>

- Patel, K. K., & Purohit, R. (2019). Improved shape memory and mechanical properties of microwave-induced shape memory polymer/MWCNTs composites. *Materials Today Communications*. <https://doi.org/10.1016/j.mtcomm.2019.100579>
- Qi, S., Fu, J., Xie, Y., Li, Y., Gan, R., & Yu, M. (2019). Versatile magnetorheological elastomer with 3D printability, switchable mechanics, shape memory, and self-healing capacity. *Composites Science and Technology*. <https://doi.org/10.1016/j.compscitech.2019.107817>
- Ramezani, M., & Monroe, M. B. B. (2022). Biostable segmented thermoplastic polyurethane shape memory polymers for smart biomedical applications. *ACS Applied Polymer Materials*, 4(3), 1956–1965. <https://doi.org/10.1021/acscapm.1c01808>
- Salimon, A. I., Senatov, F. S., Kalyaev, V., & Korsunsky, A. M. (2020). *3D and 4D printing of polymer nanocomposite materials* (pp. 161–189). Elsevier.
- Shin, E. J., Jung, Y. S., Choi, H. Y., & Lee, S. (2022a). Synthesis and fabrication of biobased thermoplastic polyurethane filament for FDM 3D printing. *Applied Polymer*, 139(40), e52959. <https://doi.org/10.1002/pen.26075>
- Shin, E. J., Park, Y. Y., Jung, Y. S., Choi, H. Y., & Lee, S. (2022b). Fabrication and characteristics of flexible thermoplastic polyurethane filament for fused deposition modeling three-dimensional printing. *Polymer Engineering and Science*, 62(9), 2947–2957. <https://doi.org/10.1002/pen.26075>
- Song, J. J., Chang, H. H., & Naguib, H. E. (2015a). Biocompatible shape memory polymer actuators with high force capabilities. *European Polymer Journal*, 67, 186–198. <https://doi.org/10.1016/j.eurpolymj.2015.03.067>
- Song, J. J., Chang, H. H., & Naguib, H. E. (2015b). Design and characterization of biocompatible shape memory polymer(SMP) blend foams with a dynamic porous structure. *Polymer*, 56, 82–92. <https://doi.org/10.1016/j.polymer.2014.09.062>
- Sun, L., Huang, W. M., Wang, C. C., Ding, Z., Zhao, Y., Tang, C., & Gao, X. Y. (2013). Polymeric shape memory materials and actuators. *Liquid Crystals*, 41(3), 277–289. <https://doi.org/10.1080/02678292.2013.805832>
- Wang, Y., Wang, Y., Liu, M., Wei, Q., & Du, B. (2022). 4D printing light-/thermo-responsive shape memory composites based on thermoplastic polyurethane/poly(lactic acid)/polyaniline blends. *High Performance Polymers*. <https://doi.org/10.1177/09540083221135499>
- Xie, T. (2011). Recent advances in polymer shape memory. *Polymer*, 52(22), 4985–5000. <https://doi.org/10.1016/j.polymer.2011.08.003>
- Zeng, B., Li, Y., Wang, L., Zheng, Y., Shen, J., & Guo, S. (2020). Body temperature triggered shape-memory effect via toughening sustainable poly(propylene carbonate) with thermoplastic polyurethane: Toward potential application of biomedical stents. *ACS Sustainable Chemistry & Engineering*, 8, 1538–1547. <https://doi.org/10.1021/acscuschemeng.9b06080>

Publisher's Note

Springer Nature remains neutral with regard to jurisdictional claims in published maps and institutional affiliations.

Imjoon Jung Graduate student, Department of Fashion and Textiles, Dong-A University, Busan 49315, Republic of Korea.

Sunhee Lee Professor, Department of Fashion Design, Dong-A University, Busan 49315, Republic of Korea.

Submit your manuscript to a SpringerOpen[®] journal and benefit from:

- Convenient online submission
- Rigorous peer review
- Open access: articles freely available online
- High visibility within the field
- Retaining the copyright to your article

Submit your next manuscript at ► [springeropen.com](https://www.springeropen.com)
